Published in final edited form as:

ACS Chem Biol. 2022 September 16; 17(9): 2605–2618. doi:10.1021/acschembio.2c00527.

Proximity Labeling Reveals Spatial Regulation of the Anaphase-Promoting Complex/Cyclosome by a Microtubule Adaptor

Xiaofu Cao,
Department of Chemistry and Chemical Biology, Cornell University, Ithaca, New York 14850, United States; Weill Institute for Cell and Molecular Biology, Cornell University, Ithaca, New York 14850, United States;

Adnan Shami Shah,
Department of Chemistry and Chemical Biology, Cornell University, Ithaca, New York 14850, United States; Weill Institute for Cell and Molecular Biology, Cornell University, Ithaca, New York 14850, United States

Ethan J. Sanford,
Weill Institute for Cell and Molecular Biology and Department of Molecular Biology and Genetics, Cornell University, Ithaca, New York 14850, United States

Marcus B. Smolka,
Weill Institute for Cell and Molecular Biology and Department of Molecular Biology and Genetics, Cornell University, Ithaca, New York 14850, United States;

Jeremy M. Baskin
Department of Chemistry and Chemical Biology, Cornell University, Ithaca, New York 14850, United States; Weill Institute for Cell and Molecular Biology, Cornell University, Ithaca, New York 14850, United States;

Abstract

The anaphase-promoting complex/cyclosome (APC/C) coordinates advancement through mitosis via temporally controlled polyubiquitination events. Despite the long-appreciated spatial organization of key events in mitosis mediated largely by cytoskeletal networks, the spatial

Corresponding Author: Jeremy M. Baskin – Department of Chemistry and Chemical Biology, Cornell University, Ithaca, New York 14850, United States; Weill Institute for Cell and Molecular Biology, Cornell University, Ithaca, New York 14850, United States; jeremy.baskin@cornell.edu.

Author Contributions

Conceptualization–X.C., A.S., and J.M.B.; funding acquisition–M.B.S. and J.M.B.; investigation–X.C., A.S., and E.J.S.; project administration–M.B.S. and J.M.B.; supervision–M.B.S. and J.M.B.; writing–original draft–X.C. and J.M.B.; writing–review and editing–X.C., A.S., E.J.S., M.B.S., and J.M.B.

Supporting Information

The Supporting Information is available free of charge at https://pubs.acs.org/doi/10.1021/acschembio.2c00527.
Additional domain mapping of the PLEKHA5–APC/C interaction and PLEKHA5 expression-level western blots, control immunofluorescence experiments for MT-TurboID, validation of APC/C enrichment by anti-ANAPC3 IP and in vitro ubiquitination assay, cell cycle analysis by propidium iodide (PI) staining and western blot using siPLEKHA5 #2, microscopy images of mitosis duration imaging, G2/M transition imaging data, CDK1 AF mutant experimental data, transduction efficiency imaging for rescue experiments, siRNA duplex sequences, reagents used in the study, and extended experimental procedures (PDF)
Raw data from SILAC mass spectrometry experiments (XLSX)

Complete contact information is available at: https://pubs.acs.org/10.1021/acschembio.2c00527

The authors declare no competing financial interest.

regulation of APC/C, the major mitotic E3 ligase, is poorly understood. We describe a microtubule-resident protein, PLEKHA5, as an interactor of APC/C and spatial regulator of its activity in mitosis. Microtubule-localized proximity biotinylation tools revealed that PLEKHA5 depletion decreased APC/C association with the microtubule cytoskeleton, which prevented efficient loading of APC/C with its coactivator CDC20 and led to reduced APC/C E3 ligase activity. PLEKHA5 knockdown delayed mitotic progression, causing accumulation of APC/C substrates dependent upon the PLEKHA5-APC/C interaction in microtubules. We propose that PLEKHA5 functions as an adaptor of APC/C that promotes its subcellular localization to microtubules and facilitates its activation by CDC20, thus ensuring the timely turnover of key mitotic APC/C substrates and proper progression through mitosis.

Graphical Abstract

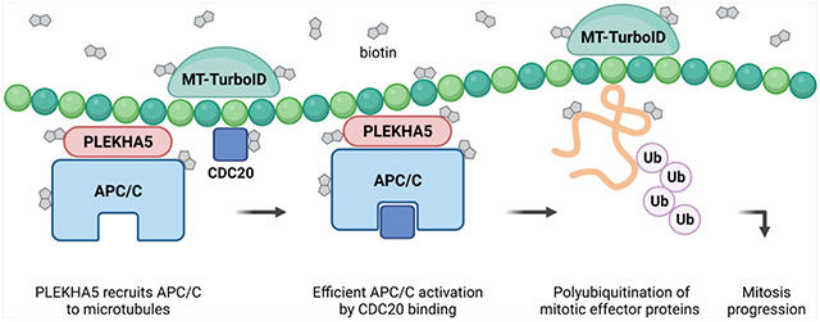

INTRODUCTION

Progression through mitosis involves spatiotemporal coordination of cytoskeletal and membrane dynamics with changes in protein activities, chromosomal dynamics, and signaling events.[1] A major role of the ubiquitin–proteasome system is to orchestrate cell cycle progression through temporally controlled protein degradation programs.[2] The anaphase-promoting complex/cyclosome (APC/C) is the primary E3 ubiquitin ligase controlling mitotic events including G2/M transition, early mitosis, the metaphase–anaphase transition, and mitotic exit.[3]

APC/C is a 14-subunit complex and conserved member of the Cullin-RING E3 ligase family that mediates K11- and K48-linked polyubiquitination of several proteins involved in mitotic progression,[4] including the cyclin-dependent kinase inhibitor p21 and cyclin A in early mitosis, cyclin B1 and the separase inhibitor securin at the metaphase–anaphase transition, and the DNA replication inhibitor geminin in early G1.[5–9] Its ubiquitin ligase activity requires the association of one of two structurally related coactivators, CDC20 and CDH1, which interacts with APC/C during mitosis and in G1 phase, respectively.[10] The temporal control of APC/C-mediated ubiquitination in these processes is well established, including identities of ubiquitination substrates and accessory factors that modulate E3 ligase activity.[11,12] However, there are major open questions concerning the spatial organization of the APC/C.[11] These include an incomplete understanding of its subcellular localizations, what factors influence changes in its localization, and how compartmentalization of APC/C at different subcellular locations affects its activity toward specific substrates.

PLEKHA5 (pleckstrin homology domain-containing family A, member 5) is a microtubule-localized protein and member of the PLEKHA4–7 family, several of which function as adaptor proteins that can regulate the subcellular localizations and thus biological functions of other proteins or protein complexes. For example, PLEKHA7 localizes to adherens junctions and recruits PDZD11 (PDZ domain-containing protein 11) to these junctions.[13] The PLEKHA7–PDZD11 complex can stabilize the plasma membrane localization and modulate the functions of multiple transmembrane proteins, including nectins for junctional integrity and the Menkes copper ATPase and the plasma membrane calcium ATPase to maintain intracellular ion homeostasis.[13–15] Furthermore, we recently showed that PLEKHA4 functions as a plasma membrane adaptor to sequester the Cullin-3 E3 ubiquitin ligase adaptor KLHL12, thus elevating Dishevelled levels and enhancing the strength of Wnt signaling pathways in Wnt-receiving cells.[16]

Here, we identified a link between the spatial organization of APC/C and the cellular functions of PLEKHA5 as a microtubule adaptor protein. The incomplete understanding of the spatial organization of APC/C is partly due to the challenges associated with effectively determining the subcellular localizations of this large, multi-subunit protein complex with conventional imaging methods. The deficiencies of these conventional tools motivated us to develop an alternative strategy harnessing TurboID-based proximity labeling[17–19] to assess APC/C localization, and we reveal a general mechanism by which the spatial organization of APC/C is coordinated by PLEKHA5 to ensure its proper activity during mitosis. We propose that PLEKHA5 functions as a microtubule-specific APC/C adaptor to recruit a pool of APC/C to the microtubule cytoskeleton, promoting its loading with CDC20 and enabling the APC/C^{CDC20}-mediated ubiquitination of key mitotic effector proteins, thus facilitating mitosis progression. In this model, PLEKHA5 regulates APC/C subcellular localization and thus accelerates its access to a critical coactivator required for its functions in mitosis, effectively reducing a 3D search in the cytosol to a 1D search along microtubule tracks. This model establishes a framework for understanding how the spatial organization of the APC/C impacts its ubiquitination activity and roles in promoting mitotic progression. Furthermore, our study establishes a set of “in vivo biochemistry”-based TurboID tools for interrogating the microtubule-associated proteome, highlighting the versatility of proximity labeling methods for examining unresolved questions in cell biology.

RESULTS AND DISCUSSION

PLEKHA5 Localizes to Microtubules via Its N-Terminal Tandem WW Domain.

We began this study by focusing on the molecular and cellular properties of PLEKHA5 as part of a larger undertaking to explore the roles of how putative phosphoinositide-binding proteins might link lipid binding to the regulation of cell signaling, and in particular, ubiquitination pathways. Toward this effort, we have centered on poorly characterized members of the PLEKHA subfamily of pleckstrin homology domain-containing proteins. Previously, we found that PLEKHA4/kramer regulates Wnt signaling pathways in mammalian cells and in *Drosophila* and promotes proliferation in melanoma by antagonizing the polyubiquitination of Dishevelled by the Cullin 3–KLHL12 E3 ligase.[16,20] The PLEKHA4 paralog PLEKHA5 shares a similar multi-domain architecture (Figure 1A)

and has been linked to proliferation and metastasis in several disease models,[21–23] although underlying mechanisms remained unknown, prompting us to investigate its molecular properties and cellular functions.

We first examined the cellular localization of PLEKHA5. Unlike PLEKHA4, which localizes to the plasma membrane,[16] endogenous PLEKHA5 was detected predominantly along the microtubule network in HeLa cells by immunofluorescence (Figures 1B and S1A) and imaging of green fluorescent protein (GFP)-tagged full-length PLEKHA5 (EGFP-PLEKHA5^{FL}, Figures 1C and S1B). As a member of the WW-PLEKHA subfamily of proteins,[14] PLEKHA5 contains two N-terminal WW domains absent from PLEKHA4. We hypothesized that the microtubule localization of PLEKHA5 might be mediated by its tandem WW domains. Indeed, we found that a GFP-tagged PLEKHA5 construct lacking the two WW domains failed to localize to microtubules and a GFP fusion to the tandem WW domains localized to microtubules similar to the full-length protein (Figure 1C). These data indicate that the tandem WW domain is necessary and sufficient to recruit PLEKHA5 to the microtubule network. These observations are consistent with recent studies demonstrating that the tandem WW domain of PLEKHA5 associates with PDZD11 and that this interaction was crucial for PLEKHA5 to localize to the microtubule network.[14,24]

PLEKHA5 Interacts with APC/C, a Key E3 Ubiquitin Ligase Regulating Mitosis.

To explore the molecular functions of PLEKHA5, we identified potential protein–protein interaction partners using stable isotope labeling by amino acids in cell culture (SILAC)-based quantitative mass spectrometry. We performed anti-GFP immunoprecipitation (IP) from HeLa cells stably expressing EGFP-PLEKHA5 or EGFP and subjected the immunoprecipitates to bottom-up proteomics analysis. Interestingly, among the most strongly enriched proteins were several subunits of the anaphase-promoting complex/cyclosome (APC/C) (Figure 1D and Table S1).

We validated the interaction of endogenous PLEKHA5 with two representative APC/C subunits, ANAPC4 and ANAPC8, by co-IP, followed by western blotting (Figure 1E,F). To map the interacting regions, we performed co-IP of APC/C subunits with several GFP-tagged constructs corresponding to truncated forms of PLEKHA5 or isolated PLEKHA5 domains (Figures 1G and S1C). The GFP fusion to the proline-rich domain (PRD) (EGFP-PLEKHA5^{PRD}) exhibited a strong interaction with APC/C (Figure 1G), whereas a construct lacking the PRD (EGFP-PLEKHA5$^{\Delta PRD}$), despite its high expression levels, failed to interact with APC/C (Figure S1C). These results suggest that the PRD of PLEKHA5 is sufficient and necessary for the interaction with APC/C.

One consequence of the PLEKHA5–APC/C interaction could be that PLEKHA5 is a ubiquitination substrate of APC/C. To test this possibility, we monitored PLEKHA5 protein levels over the cell cycle by western blotting in HeLa cells that were first synchronized to the S-phase by double thymidine block (DTB)[25] and then released from synchronization, with samples collected every 2 h for 24 h (Figure S1D). Unlike other known protein substrates of APC/C, such as cyclin A and cyclin B1, which show oscillating expression patterns, PLEKHA5 protein levels were remarkably stable over the experimental timeframe

(Figure S1E,F), indicating that PLEKHA5 levels are not regulated via cell cycle-dependent proteolysis and thus that PLEKHA5 is likely not an APC/C substrate.

Development of a Proximity Biotinylation Tool to Probe the Microtubule Localization of Endogenous PLEKHA5, APC/C, and Its Substrates.

If PLEKHA5 is not a ubiquitination substrate of APC/C, we next hypothesized that it may function as an adaptor protein to recruit this E3 ligase to the microtubule network as a site of action because the microtubule cytoskeleton is a major cellular structure that organizes mitotic events. To test this hypothesis, we needed to examine the colocalizations of PLEKHA5, APC/C, CDC20, and the substrates on microtubules. Previous studies using immunofluorescence have reported multiple localizations of APC/C, including the cytosol, the prophase nucleus, and, critically, numerous parts of the microtubule network, including spindle poles/centrosomes, kinetochores, and chromosomes.[11,26–28] However, commercially available antibodies for different APC/C subunits have failed to consistently mark the subcellular localizations of the complex by immunofluorescence, and exogenous overexpression of GFP fusions to individual APC/C subunits may not reliably assemble into functional APC/C complexes.[27,29] A recent high-throughput effort (OpenCell) has generated CRISPR knock-in cell lines with GFP fusions to >1300 human proteins expressed endogenously,[30] yet for several APC/C subunits in this collection, no reliable localization was observed to intracellular organelles or structures.

Fortunately, recent developments of enzyme-mediated proximity labeling techniques such as BioID/TurboID and APEX provide new avenues for mapping the subcellular localizations of untagged, endogenous proteins with near-nanometer spatial resolution.[31] In these strategies, an organelle-tethered enzyme releases a highly reactive intermediate, typically a biotin derivative, enabling covalent biotinylation of nearby proteins within a limited radius. As such, proximity biotinylation has been widely applied for mapping the proteomes of organelles and other discrete structures such as membrane contact sites and synaptic clefts. Notably, the covalent nature of the labeling allows for sensitive detection and quantification of even minor or transient spatially restricted pools of proteins that exhibit dynamic behavior and/or can exist in multiple subcellular localizations, including large cytosolic pools, all of which are very challenging to visualize with standard imaging-based methods.

Therefore, we developed an alternative strategy harnessing TurboID-based proximity labeling[17,19,32] to ascertain the microtubule localization of endogenous PLEKHA5, APC/C, and other proteins (Figure 2A). Proximity labeling-based tools exist for tagging specific subsets of the microtubule network, for example, the centrosome–cilium interface, noncentrosomal microtubule organizing centers, kinetochores, and dynein-associated proteins.[33–36] To our knowledge, however, tools for broad labeling of proteins associated with the microtubule network in mammalian cells were not available. Therefore, we developed two microtubule-targeted TurboID (MT-TurboID) constructs by fusing V5-tagged TurboID to two microtubule-associated proteins: doublecortin (DCX) and the microtubule-binding domain of ensconsin/MAP7 (EMTB).[37,38]

We first validated the localization and biotinylation activity of the two MT-TurboID constructs, DCX-TurboID-V5 and EMTB-TurboID-V5, by performing IF against the V5

tag and biotin (Figure 2B–E and Figure S2). We then validated the specificity of the MT-TurboIDs using streptavidin-agarose enrichment of biotinylated proteins, followed by western blot analysis (Figure 2F,G). Both MT-TurboID constructs successfully labeled microtubule-associated protein 4 (MAP4), α-tubulin, and PLEKHA5 upon the addition of exogenous biotin but showed negligible biotinylation of markers of the plasma membrane (CD44), the actin cytoskeleton (actin), and the nucleus (histone H3), demonstrating that the activity of MT-TurboIDs was selectively confined to proteins on microtubules. Importantly, in the same experiment, representative APC/C subunits ANAPC3, ANAPC5, and ANAPC6, the coactivator CDC20, and APC/C substrates including cyclin A, cyclin B1, p21, and securin[5–8] were biotinylated by both MT-TurboIDs in either asynchronous or prometaphase-synchronized cells by a 16 h treatment of S-trityl-L-cysteine (STLC)[39] (Figure 2F,G). These results reveal that APC/C structural subunits, CDC20, and several APC/C substrates all exhibit microtubule localization both in interphase and in M phase and further validate MT-TurboIDs as general “in vivo biochemistry” tools for interrogating the microtubule localization of target proteins of interest.

PLEKHA5 Depletion Caused a Decrease in the Microtubule Localization of APC/C Subunits but Not CDC20.

Next, to elucidate the requirement for PLEKHA5 in promoting APC/C localization to microtubules, we evaluated the extent of microtubule association of APC/C in control versus siPLEKHA5 cells using MT-TurboID proximity biotinylation, enrichment of biotinylated proteins, and western blot (Figure 3A). We confirmed that treating cells with siPLEKHA5 did not alter the expression level nor the activity of MT-Turbos in cells stably expressing these constructs (Figure 3C,E, V5 and streptavidin blots). Upon knockdown of PLEKHA5 in either asynchronous populations or cells synchronized to prometaphase, several representative subunits of the APC/C complex exhibited a significant decrease in microtubule localization marked by both MT-TurboID constructs (Figure 3B–E). However, in these same experiments, there was no significant change in levels of microtubule-associated CDC20 upon PLEKHA5 knockdown (Figure 3B–E). These data suggest that PLEKHA5 plays a role in the recruitment of a pool of apo APC/C complexes to microtubules and are consistent with the hypothesis, wherein PLEKHA5 functions as an APC/C adaptor to promote its localization to microtubules.

PLEKHA5 Promotes APC/C Association with CDC20 and Activation in Prometaphase.

Based on the above data showing decreased microtubule-associated APC/C but not CDC20 upon PLEKHA5 depletion, we tested if PLEKHA5 knockdown impairs the interaction of APC/C and CDC20 for the assembly of active E3 ligase complexes at microtubules and thus affects its catalytic activity. We first examined the composition of APC/C in mitosis. We isolated endogenous APC/C via anti-ANAPC3 IP from HeLa cells that were either asynchronous or synchronized to prometaphase by STLC, and we confirmed that several representative structural subunits and its key mitotic coactivator CDC20 were enriched from the cell lysates (Figure S3A). We then compared the APC/C enriched from prometaphase cells that had been transfected with control or two different PLEKHA5 siRNA duplexes (Figure 4A). PLEKHA5 knockdown did not affect the assembly of the structural components of APC/C, but the association of APC/C with CDC20 was significantly

reduced, although the overall level of CDC20 was not affected by siPLEKHA5 treatment (Figures 4B,C and S3B,C).

The reduced APC/C–CDC20 interaction was rescued upon expression of an siRNA-resistant EGFP-PLEKHA5^{FL} construct, but minimal rescue was observed using two truncation constructs, EGFP-PLEKHA5$^{\Delta WW}$ or EGFP-PLEKHA5$^{\Delta PRD}$ (Figure 4E–G). EGFP-PLEKHA5$^{\Delta WW}$ retained its interaction with APC/C (Figure S1C) yet could not localize to the microtubule network (Figure 1C), whereas EGFP-PLEKHA5$^{\Delta PRD}$ localized to microtubules correctly (Figure 4D) but failed to interact with APC/C (Figure S1C). The results from these rescue experiments demonstrate that both the microtubule localization of PLEKHA5 and its interaction with APC/C are critical to restoring normal APC/C–CDC20 association in prometaphase cells that is perturbed upon PLEKHA5 knockdown. These data indicate that the recruitment of a pool of APC/C to microtubules by PLEKHA5 promotes efficient loading of CDC20 onto APC/C to form active E3 ligase complexes.

To measure the effect of this decreased CDC20 association on APC/C function, we assessed the E3 ligase activity of APC/C^{CDC20} using in vitro ubiquitination assays.[40] We reconstituted the ubiquitination cascade using the enriched APC/C and other required components, including E1, E2s, ubiquitin, ATP, and recombinantly purified securin as the APC/C substrate. Western blot analysis of the reaction mixtures revealed that the in vitro ubiquitination of securin was dependent upon the presence of all components, and the APC/C purified by IP was indeed active (Figure S3D). Next, we evaluated the catalytic activities of APC/C^{CDC20} purified from control or siPLEKHA5 cells synchronized to prometaphase. Upon PLEKHA5 knockdown, the in vitro polyubiquitination of securin by APC/C was significantly decreased, which was consistent with a decrease in APC/C loading with CDC20 caused by siPLEKHA5 (Figure 4H,I). These results indicate that depletion of PLEKHA5 from prometaphase cells antagonizes the loading of CDC20 onto APC/C and thus impairs the catalytic activity of the E3 ubiquitin ligase toward its substrates.

PLEKHA5 Knockdown Attenuates Mitotic Progression and Causes Increases in the Fraction of Cells in G2 and M Phases.

The modulation of APC/C activity by PLEKHA5 suggests potential functions of PLEKHA5 in mitosis, as APC/C is the primary E3 ligase controlling mitotic entry, progression, and exit. We monitored mitosis progression by performing temperature- and CO_2-controlled live-cell imaging over extended time periods of asynchronous cells expressing fluorescent markers of chromatin, H2B-mCherry, and quantified the time from nuclear envelope breakdown (NEBD) to anaphase onset, signified by chromosomal segregation[41] (Figure 5A). PLEKHA5 knockdown caused a minor but significant increase in time for cells to enter anaphase (Figures 5B and S4A). The modest nature of this delay suggests an effect of PLEKHA5 on only a subset of APC/C complexes. Nevertheless, we note that the effect on mitosis in unperturbed, asynchronous cells seen here is similar in magnitude to depletion of the protein phosphatase PP2A-B55, a nonessential but important regulator of mitosis.[41]

We also analyzed the cell-cycle phase of HeLa cells subject to DTB synchronization and release by using propidium iodide staining of fixed cells, followed by flow cytometry (Figure 5C). We found that depletion of PLEKHA5 by two different siRNAs led to an

increased percentage of cells retained in G2 and M phases after release from DTB (Figures 5D–F and S4B–D).

PLEKHA5 Knockdown Increases the Levels of Mitotic APC/C Substrates.

To further understand the effect of PLEKHA5 knockdown in APC/C-mediated polyubiquitination and mitosis progression on a molecular level, we analyzed the protein levels of several APC/C ubiquitination substrates and mitosis markers following DTB synchronization and release via western blotting (Figure 6A). Consistent with previous results wherein APC/C isolated from siPLEKHA5-treated cells exhibited lower in vitro catalytic activity, several APC/C substrates, including cyclin A, cyclin B1, securin, and p21, all showed aberrant accumulation upon PLEKHA5 knockdown using two different siRNA duplexes (Figures 6B,C and S4E,F). These results indicate that PLEKHA5 depletion results in a defect in APC/C-mediated polyubiquitination of mitotic effector proteins and subsequent proteasomal degradation.

However, the substantial accumulation of p21 at early timepoints caught our attention because p21, in addition to being an APC/C substrate, is also an inhibitor of the CDK1–cyclin B1 complex, the major kinase complex that positively regulates mitosis onset and advance.[42] The accumulation of p21 may be due to insufficient APC/C activity, but it can also suggest the activation of the G2/M DNA damage checkpoint, which leads to prolonged G2/M arrest.[43] Thus, we analyzed the levels of a mitosis protein marker, phospho-histone H3 at serine 10 (H3 S10p), and CDK1. PLEKHA5 knockdown caused a delay in the appearance and the peak expression of H3 S10p (Figures 6B,C and S4E,F). Furthermore, the analysis of CDK1 revealed prolonged expression of its inactive form, which bore inhibitory phosphorylation at tyrosine 15 (CDK1 Y15p),[44] at later timepoints in PLEKHA5-depleted cells compared to the control (Figures 6B,C and S3E,F). These results, along with the induction of p21 expression, indicate that siPLEKHA5 potentially caused a partial G2-to-M transition arrest prior to its function in mitosis and that PLEKHA5 may play additional roles in cell cycle regulation beyond a role in mitosis.

To explore the potential effects of PLEKHA5 depletion prior to mitotic entry, we analyzed the G2-to-M transition by imaging cells expressing GFP-tagged proliferating cell nuclear antigen (EGFP-PCNA) and H2B-mCherry and measuring the time between the disappearance of PCNA puncta and NEBD[45] (Figure S5A). In the asynchronous population of cells, we found no statistically significant difference between siPLEKHA5 and control in the G2-to-M transition period (Figure S5B,C). Additionally, we examined the levels of the same G2/M markers and APC/C substrates after a DTB synchronization and release but in the presence of the phosphodeficient CDK1 T14A/Y15F (AF) mutant (Figure S5D). This CDK1 AF mutant, which cannot possess inhibitory phosphorylation marks, is constitutively active, and its expression induces cells to partially bypass the G2/M checkpoint.[44,46–48] Compared to control, cells expressing CDK1(AF)-3xFLAG with control siRNA treatment showed increased mitosis progression, signified by earlier timepoints for H3 S10p peak expression, a faster decrease in its levels, and reduced accumulation of APC/C substrates (Figure S5E,F, compare the gray and black lines in quantification plots, significance marked by *). These results confirm that expressing the CDK1(AF) mutant indeed permits cells

to partially bypass the G2/M checkpoint and promote mitosis entry in our system. We then compared the effect of PLEKHA5 knockdown versus control siRNA in CDK1(AF)-expressing cells. Again, we observed a delay in H3 S10p disappearance and elevated levels of endogenous CDK1 Y15p and APC/C substrates upon PLEKHA5 knockdown (Figure S5E,F, compare the black and red lines in quantification plots, significance marked by #). Collectively, these studies support a major role for PLEKHA5 in regulating mitosis.

Interaction of PLEKHA5 with APC/C at Microtubules Is Required to Rescue Mitotic Defects Caused by PLEKHA5 Knockdown.

To further investigate the mechanism of the PLEKHA5–APC/C interaction in regulating mitosis, we performed rescue experiments with siPLEKHA5-resistant EGFP, EGFP-PLEKHA5^{FL}, EGFP-PLEKHA5$^{\Delta WW}$, and EGFP-PLEKHA5$^{\Delta PRD}$ constructs (Figure 7A). In accordance with previous results, control rescue (with EGFP) in siPLEKHA5-treated cells led to a significant increase of APC/C substrates and G2- and M-phase protein markers (Figure 7B,C, compare the first and second bands in groups of five in representative blots, e.g., lanes 16 vs 17, and the black and red lines in quantification plots, significance marked by *). Importantly, the changes in protein expression patterns induced by PLEKHA5 depletion were partially restored by the introduction of an siRNA-resistant form of full-length PLEKHA5 protein (Figure 7B,C, compare the second and third bands in groups of five in representative blots, e.g., lanes 17 vs 18, and the red and dark-green lines in quantification plots, significance marked by #). For example, the peak expression of H3 S10p shifted earlier to 9 h post-release, and its levels decreased to a greater extent at later time points. Similarly, the buildup of other markers and APC/C substrates was partially reduced by the expression of EGFP-PLEKHA5^{FL} in cells treated with siPLEKHA5.

We note that complete rescue was not achieved, likely due to both the relatively poor expression of EGFP-PLEKHA5^{FL} and the maximal transduction efficiency with the rescue construct of ~60% (Figure S6). Nevertheless, minimal rescue was observed in cells expressing siRNA-resistant forms of the truncation constructs, EGFP-PLEKHA5$^{\Delta WW}$ or EGFP-PLEKHA5$^{\Delta PRD}$, which are unable to recruit APC/C to microtubules, despite their much higher expression in rescue experiments compared to the full-length construct (Figure 7B,C, compare the second and fourth or fifth bands in groups of five in representative blots, e.g., lanes 17 vs 19 and 20, and the red and yellow–green or blue–green lines in quantification plots, significance marked by † and ‡, respectively, and Figure S6). These rescue experiments reveal that the recruitment of APC/C to microtubules by PLEKHA5 is critical for the proteolysis of APC/C ubiquitination substrates and proper advancement of mitosis. Collectively, even though we cannot fully exclude the possibility that PLEKHA5 exerts additional regulation of the cell cycle prior to mitosis, which will be discussed further, our data suggest that PLEKHA5 ensures proper mitotic progression by recruiting a pool of APC/C complexes to microtubules and are consistent with a model wherein PLEKHA5 functions as an APC/C adaptor to promote its localization to microtubules and thus enhance the efficiency of CDC20 loading onto this pool of APC/C to promote substrate ubiquitination during mitosis (Figure 8).

PLEKHA5 belongs to the PLEKHA4–7 protein family, members of which serve as intracellular adaptor proteins to promote specific subcellular localization of their interacting proteins to carry out various functions.[13,16] PLEKHA5 is critical for proliferation and invasiveness of melanoma cells with a high propensity for brain metastasis.[21] Other studies have implicated PLEKHA5 in the regulation of malignant progression in diffuse-type gastric carcinoma and breast cancer metastasis.[22,23] These reports underscore the importance of elucidating the fundamental molecular and cellular functions of PLEKHA5, particularly those that impact the regulation of the cell cycle.

We found that PLEKHA5 exhibits a microtubule localization in HeLa cells and interacts with the E3 ubiquitin ligase APC/C. We reasoned that PLEKHA5 is likely not a substrate for APC/C during mitosis because PLEKHA5 levels remained stable throughout the cell cycle, and it does not possess APC/C destruction motifs such as the D-box, KEN-box, or ABBA motif[49] within its primary amino acid sequence. Instead, we hypothesized that PLEKHA5 might be a microtubule-localized APC/C adaptor.

To overcome the challenges associated with determining APC/C localization through imaging and to test the hypothesis that PLEKHA5 mediates the spatial organization of APC/C, we developed a proximity biotinylation approach using microtubule-targeted TurboID constructs to assess endogenous protein localizations to the microtubule cytoskeleton. Indeed, we detected biotinylation of PLEKHA5, APC/C, CDC20, and relevant APC/C substrates, confirming that these proteins localize to or very near to microtubules. The recruitment of APC/C to microtubules was partly dependent on PLEKHA5, as PLEKHA5 depletion reduced microtubule-associated APC/C and further impaired the loading of CDC20 onto this pool of APC/C and exhibited a decrease in catalytic activity.

The connection to APC/C prompted us to explore the potential roles of PLEKHA5 in regulating mitosis. Depletion of PLEKHA5 antagonized mitotic progression and led to accumulations of APC/C^{CDC20} substrates in a manner dependent upon the PLEKHA5–APC/C interaction at microtubules. Unexpectedly, we also observed a delay in mitotic entry from the DTB experiment, although the analysis of G2-to-M transition in asynchronous HeLa cells by imaging showed little difference in control versus siPLEKHA5 cells. Still, the induction of high p21 expression may indicate the presence of DNA damage upon PLEKHA5 knockdown. One possible explanation involves CDH1, the coactivator for APC/C from mitotic exit to the end of G1. Our proposed model of PLEKHA5 as a microtubule adaptor protein for APC/C also applies, in principle, to facilitate the formation of the active APC/C^{CDH1} complex, which has been shown to respond to DNA damage and regulate DNA repair.[50] In the context of PLEKHA5 knockdown, the APC/C–CDH1 interaction may decrease and therefore impair APC/C^{CDH1} catalytic activity, similar to what we have shown for APC/C^{CDC20}, which would lead to unresolved DNA damage and activation of the checkpoint machinery to delay mitotic entry. Testing of this hypothesis will require future studies into the potential effects of PLEKHA5 on APC/C^{CDH1} activity and function.

Collectively, this study reveals a new framework for the spatial regulation of APC/C in mitosis. In our model, PLEKHA5 interacts with and recruits a pool of APC/C to the

microtubule cytoskeleton. This interaction would increase the local concentration of APC/C along the network and effectively reduce the dimensionality of its search for coactivators and substrates from three dimensions (in the cytosol) to one dimension (along microtubule tracks). Upon mitotic phosphorylation of its subunits and relief of the spindle assembly checkpoint, this pool of APC/C would efficiently encounter its coactivator CDC20 and subsequently be capable of ubiquitinating key mitotic effector proteins. Our study not only reveals a mechanism controlling the spatial regulation of the major E3 ubiquitin ligase in mitosis but also provides a means for understanding how such spatial regulation could be intimately linked to the established temporal regulation of this enzyme that is critical for progression through mitosis. Given the localization of PLEKHA5 and the large number of PLEKHA5-interacting proteins identified in our proteomics experiments, it is possible that PLEKHA5 acts more generally as an adaptor to facilitate protein recruitment to the microtubule cytoskeleton in both interphase and mitosis. Furthermore, our studies provide a mechanism that accounts for a role for PLEKHA5 in promoting progression through mitosis that may be operational in settings where elevated PLEKHA5 levels have been linked to cancer progression. Finally, the MT-TurboIDs developed herein have the potential to serve as broadly useful tools for interrogating the dynamic association of diverse proteins with the microtubule cytoskeleton in many physiological contexts.

MATERIALS AND METHODS

Cell Culture.

Flp-In T-Rex HeLa (Thermo Fisher) and HEK 293TN cells (Anthony Bretscher, Cornell University) were cultured in DMEM (Corning) supplemented with 10% fetal bovine serum (FBS) (Corning) and 1% penicillin/streptomycin (P/S, Corning) at 37 °C in a 5% CO_2 atmosphere. HEK 293TN cells were also supplemented with 1% sodium pyruvate (Corning). Stable expression of the protein of interest was achieved following the published procedures. For more details, please refer to the Supporting Information. Cell lines were used without further authentication, and mycoplasma testing (MycoSensor PCR assay, Agilent) was performed yearly.

Confocal Microscopy.

Live-cell imaging and immunofluorescence were performed as previously described.[16] More details are included in the Supporting Information. Images were acquired via Zeiss Zen Blue 2.3 software using a Zeiss LSM 800 confocal laser scanning microscope equipped with Plan Apochromat objectives (40× 1.4 NA) and two GaAsP PMT detectors. Solid-state lasers (405, 488, and 561 nm) were used to excite DAPI, EGFP/Alexa Fluor 488, and mCherry/Alexa Fluor 568, respectively. Live-cell time-series movies were acquired using Definite Focus. Depending on the experiments, images and movies were acquired either at room temperature or at 37 °C with a 5% CO_2 atmosphere. Acquired images were analyzed using FIJI.

SILAC Labeling and Mass Spectrometry-Based Proteomics Analysis.

For quantitative proteomics, Flp-In HeLa cells stably expressing EGFP-PLEKHA5 were cultured in “heavy” SILAC DMEM media (Thermo) supplemented with 10% dialyzed

FBS (Corning) and 1% P/S for at least five passages to allow full labeling of cells before they were used in experiments. “Light” EGFP-expressing HeLa cell line was generated previously.[16] “Heavy” SILAC DMEM contained L-lysine $^{13}C_6$, $^{15}N_2$ and L-arginine $^{13}C_6$, $^{15}N_4$. “Light” SILAC DMEM contained L-lysine $^{12}C_6$, $^{14}N_2$ and L-arginine $^{12}C_6$, $^{14}N_4$. Cells were lysed and immunoprecipitated with GFP-Trap magnetic agarose and processed for mass spectrometry following published procedures.[51,52] More details about the procedures and the complete list of PLEKHA5 interactors are available in the Supporting Information.

Proximity Biotinylation by MT-TurboIDs.

HeLa cells transfected with pCDNA3-DCX-TurboID-V5 or pCDNA3-EMTB-TurboID-V5 for 30 h were incubated with 500 μM biotin for 10 min at 37 °C under 5% CO_2. For localization by immunofluorescence, cells were rinsed five times with 1× PBS and processed for immune-fluorescence analysis as described earlier (see the Confocal Microscopy section). For streptavidin-agarose pulldown and western blot, cells were rinsed five times with 1× PBS and lysed with RIPA buffer supplemented with cOmplete™ Protease Inhibitor Cocktail (Roche). Cell lysates were sonicated with four pulses at 20% intensity and centrifuged at 13,000*g* for 5 min at 4 °C. The protein concentration of the clarified cell lysates was quantified using the bicinchoninic acid (BCA) assay (Thermo Fisher), and a small fraction of the clarified cell lysates was reserved and normalized as input. The remaining cell lysates were subjected to immunoprecipitation using streptavidin-agarose (Thermo Fisher) with rotation at 4 °C overnight. The resin was then centrifuged for 5 min at 1000*g*, washed two times with RIPA buffer, one time with 1 M KCl, one time with 0.1 M Na_2CO_3, one time with 2 M urea in 10 mM Tris pH 8.0, and two times with RIPA buffer to eliminate nonspecific binding. Samples were then denatured and analyzed by SDS-PAGE and western blot with detection by chemiluminescence using the Clarity Western ECL substrate.

Cell Synchronization.

S-Phase synchronization by DTB and prometaphase synchronization by STLC were performed following published procedures with slight modifications, as described in the Supporting Information.[25,40]

Cell Cycle Analysis.

Assays to analyze cell-cycle phases were performed as previously described, as described in the Supporting Information.

Isolation of Endogenous APC/C and In Vitro Ubiquitination Assays.

Enrichment of APC/C^{CDC20} and the in vitro ubiquitination assay were done following published protocol with slight modifications,[40] as described in the Supporting Information.

Statistical Analysis.

For all experiments involving quantification, statistical significance was calculated using an unpaired two-tailed Student’s *t*-test with unequal variance in Microsoft Excel, a Mann–Whitney *U* test and a Kolmogorov–Smirnov test in GraphPad Prism, or a one-way ANOVA

with Tukey post-hoc test in GraphPad Prism, as indicated in figure legends. Statistical significance of $p < 0.05$ or lower is reported, and the number of biological replicates analyzed is stated in figure legends. All raw data were plotted into graphs using GraphPad Prism. In figures containing scatter plots with straight connecting lines between markers to show changes in measurement over time, the mean at each timepoint was plotted, and the error bars represent the standard deviation. For regular scatter plots, the black line indicates the mean, and each dot represents an individual biological replicate.

Supplementary Material

Refer to Web version on PubMed Central for supplementary material.

ACKNOWLEDGMENTS

We acknowledge support from the NIH (J.M.B.: R01GM131101 and R01GM143367; M.B.S. : R35GM141159) and the Sloan Foundation (J.M.B.: Sloan Research Fellowship). We thank R. Tei, W. Cao, and R. Zaman for technical assistance, the Bretscher lab for the HEK 293TN cell line, the Yu lab for the PLEKHA5 cDNA, the Lammerding lab for the pCDH-CMV-MCS-EF1α-Puro plasmid, the Fromme and Emr labs for equipment, and I. Cheeseman, M. Goldberg, and members of the Baskin lab for helpful discussions.

REFERENCES

(1). Morgan DO The Cell Cycle: Principles of Control; New Science Press Ltd: London, 2006.

(2). Rape M Ubiquitylation at the Crossroads of Development and Disease. Nat. Rev. Mol. Cell Biol 2018, 19, 59–70. [PubMed: 28928488]

(3). Pines J Cubism and the Cell Cycle: The Many Faces of the APC/C. Nat. Rev. Mol. Cell Biol 2011, 12, 427–438. [PubMed: 21633387]

(4). Yau RG; Doerner K; Castellanos ER; Haakonsen DL; Werner A; Wang N; Yang XW; Martinez-Martin N; Matsumoto ML; Dixit VM; et al. Assembly and Function of Heterotypic Ubiquitin Chains in Cell-Cycle and Protein Quality Control. Cell 2017, 171, 918–933 e20. [PubMed: 29033132]

(5). Amador V; Ge S; Santamaría PG; Guardavaccaro D; Pagano M APC/CCdc20 Controls the Ubiquitin-Mediated Degradation of P21 in Prometaphase. Mol. Cell 2007, 27, 462–473. [PubMed: 17679094]

(6). Geley S; Kramer E; Gieffers C; Gannon J; Peters JM; Hunt T Anaphase-Promoting Complex/Cyclosome-Dependent Proteolysis of Human Cyclin A Starts at the Beginning of Mitosis and Is Not Subject to the Spindle Assembly Checkpoint. J. Cell Biol 2001, 153, 137–148. [PubMed: 11285280]

(7). King RW; Peters J-M; Tugendreich S; Rolfe M; Hieter P; Kirschner MWA 20S Complex Containing CDC27 and CDC16 Catalyzes the Mitosis-Specific Conjugation of Ubiquitin to Cyclin B. Cell 1995, 81, 279–288. [PubMed: 7736580]

(8). Zur A; Brandeis M Securin Degradation Is Mediated by Fzy and Fzr, and Is Required for Complete Chromatid Separation but Not for Cytokinesis. EMBO J. 2001, 20, 792–801. [PubMed: 11179223]

(9). McGarry TJ; Kirschner MW Geminin, an Inhibitor of DNA Replication, Is Degraded during Mitosis. Cell 1998, 93, 1043–1053. [PubMed: 9635433]

(10). Kimata Y; Baxter JE; Fry AM; Yamano H A Role for the Fizzy/Cdc20 Family of Proteins in Activation of the APC/C Distinct from Substrate Recruitment. Mol. Cell 2008, 32, 576–583. [PubMed: 19026787]

(11). Sivakumar S; Gorbsky GJ Spatiotemporal Regulation of the Anaphase-Promoting Complex in Mitosis. Nat. Rev. Mol. Cell Biol 2015, 16, 82–94 Nature Publishing Group January. [PubMed: 25604195]

(12). Watson ER; Brown NG; Peters JM; Stark H; Schulman BA Posing the APC/C E3 Ubiquitin Ligase to Orchestrate Cell Division. Trends Cell Biol. 2019, 29, 117–134. [PubMed: 30482618]

(13). Shah J; Guerrera D; Vasileva E; Sluysmans S; Bertels E; Citi S PLEKHA7: Cytoskeletal Adaptor Protein at Center Stage in Junctional Organization and Signaling. Int. J. Biochem. Cell Biol 2016, 75, 112–116. [PubMed: 27072621]

(14). Sluysmans S; Méan I; Xiao T; Boukhatemi A; Ferreira F; Jond L; Mutero A; Chang CJ; Citi S PLEKHA5, PLEKHA6, and PLEKHA7 Bind to PDZD11 to Target the Menkes ATPase ATP7A to the Cell Periphery and Regulate Copper Homeostasis. Mol. Biol. Cell 2021, 32, ar34. [PubMed: 34613798]

(15). Sluysmans S; Salmaso A; Rouaud F; Méan I; Brini M; Citi S The PLEKHA7-PDZD11 Complex Regulates the Localization of the Calcium Pump PMCA and Calcium Handling in Cultured Cells. J. Biol. Chem 2022, 298, 102138. [PubMed: 35714771]

(16). Shami Shah A; Batrouni AG; Kim D; Punyala A; Cao W; Han C; Goldberg ML; Smolka MB; Baskin JM PLEKHA4/Kramer Attenuates Dishevelled Ubiquitination to Modulate Wnt and Planar Cell Polarity Signaling. Cell Rep. 2019, 27, 2157–2170 e8. [PubMed: 31091453]

(17). Samavarchi-Tehrani P; Samson R; Gingras AC Proximity Dependent Biotinylation: Key Enzymes and Adaptation to Proteomics Approaches. Mol. Cell. Proteomics 2020, 19, 757–773. [PubMed: 32127388]

(18). Branon TC; Bosch JA; Sanchez AD; Udeshi ND; Svinkina T; Carr SA; Feldman JL; Perrimon N; Ting AY Efficient Proximity Labeling in Living Cells and Organisms with TurboID. Nat. Biotechnol 2018, 36, 880–887. [PubMed: 30125270]

(19). Qin W; Cho KF; Cavanagh PE; Ting AY Deciphering Molecular Interactions by Proximity Labeling. Nat. Methods 2021, 18, 133–143 2021, 18 (2). [PubMed: 33432242]

(20). Shami Shah A; Cao X; White AC; Baskin JM PLEKHA4 Promotes Wnt/β-Catenin Signaling-Mediated G1-S Transition and Proliferation in Melanoma. Cancer Res. 2021, 81, 2029–2043. [PubMed: 33574086]

(21). Jilaveanu LB; Parisi F; Barr ML; Zito CR; Cruz-Munoz W; Kerbel RS; Rimm DL; Bosenberg MW; Halaban R; Kluger Y; et al. PLEKHA5 as a Biomarker and Potential Mediator of Melanoma Brain Metastasis. Clin. Cancer Res 2015, 21, 2138–2147. [PubMed: 25316811]

(22). Liu J; Adhav R; Miao K; Su SM; Mo L; Chan UI; Zhang X; Xu J; Li J; Shu X; et al. Characterization of BRCA1-Deficient Premalignant Tissues and Cancers Identifies Plekha5 as a Tumor Metastasis Suppressor. Nat. Commun 2020, 11, 4875. [PubMed: 32978388]

(23). Nagamura Y; Miyazaki M; Nagano Y; Yuki M; Fukami K; Yanagihara K; Sasaki K; Sakai R; Yamaguchi H PLEKHA5 Regulates the Survival and Peritoneal Dissemination of Diffuse-Type Gastric Carcinoma Cells with Met Gene Amplification. Oncog 2021, 10, 25 10 (3).

(24). Sluysmans S; Méan I; Jond L; Citi S WW PH and C-Terminal Domains Cooperate to Direct the Subcellular Localizations of PLEKHA5, PLEKHA6 and PLEKHA7. Front. Cell Dev. Biol 2021, 9, 729444. [PubMed: 34568338]

(25). Ma HT; Poon RYC Synchronization of HeLa Cells. Methods Mol. Biol 2017, 1524, 189–201. [PubMed: 27815904]

(26). Tugendreich S; Tomkiel J; Earnshaw W; Hieter P CDC27Hs Colocalizes with CDC16Hs to the Centrosome and Mitotic Spindle and Is Essential for the Metaphase to Anaphase Transition. Cell 1995, 81, 261–268. [PubMed: 7736578]

(27). Acquaviva C; Herzog F; Kraft C; Pines J The Anaphase Promoting Complex/Cyclosome Is Recruited to Centromeres by the Spindle Assembly Checkpoint. Nat. Cell Biol 2004, 6, 892–898. [PubMed: 15322556]

(28). Sivakumar S; Daum JR; Tipton AR; Rankin S; Gorbsky GJ The Spindle and Kinetochore–Associated (Ska) Complex Enhances Binding of the Anaphase-Promoting Complex/Cyclosome (APC/C) to Chromosomes and Promotes Mitotic Exit. Mol. Biol. Cell 2014, 25, 594–605. [PubMed: 24403607]

(29). Huang JY; Raff JW The Dynamic Localisation of the Drosophila APC/C: Evidence for the Existence of Multiple Complexes That Perform Distinct Functions and Are Differentially Localised. J. Cell Sci 2002, 115, 2847–2856. [PubMed: 12082146]

(30). Cho NH; Cheveralls KC; Brunner A-D; Kim K; Michaelis AC; Raghavan P; Kobayashi H; Savy L; Li JY; Canaj H; et al. OpenCell: Endogenous Tagging for the Cartography of Human Cellular Organization. Science 2022, 375, No. eabi6983. [PubMed: 35271311]

(31). Zhou Y; Zou P The Evolving Capabilities of Enzyme-Mediated Proximity Labeling. Curr. Opin. Chem. Biol 2021, 60, 30–38. [PubMed: 32801087]

(32). Branon TC; Bosch JA; Sanchez AD; Udeshi ND; Svinkina T; Carr SA; Feldman JL; Perrimon N; Ting AY Efficient Proximity Labeling in Living Cells and Organisms with TurboID. Nat. Biotechnol 2018, 38, 880–887.

(33). Gupta GD; Coyaud É; Gonçalves J; Mojarad BA; Liu Y; Wu Q; Gheiratmand L; Comartin D; Tkach JM; Cheung SWT; et al. A Dynamic Protein Interaction Landscape of the Human Centrosome-Cilium Interface. Cell 2015, 163, 1484–1499. [PubMed: 26638075]

(34). Redwine WB; DeSantis ME; Hollyer I; Htet ZM; Tran PT; Swanson SK; Florens L; Washburn MP; Reck-Peterson SL The Human Cytoplasmic Dynein Interactome Reveals Novel Activators of Motility. Elife 2017, 6, No. e28257. [PubMed: 28718761]

(35). Remnant L; Booth DG; Vargiu G; Spanos C; Kerr ARW; Earnshaw WC In vitro BioID: mapping the CENP-A microenvironment with high temporal and spatial resolution. Mol. Biol. Cell 2019, 30, 1314–1325. [PubMed: 30892990]

(36). Sanchez AD; Branon TC; Cote LE; Papagiannakis A; Liang X; Pickett MA; Shen K; Jacobs-Wagner C; Ting AY; Feldman JL Proximity Labeling Reveals Non-Centrosomal Microtubule-Organizing Center Components Required for Microtubule Growth and Localization. Curr. Biol 2021, 31, 3586–3600 e11. [PubMed: 34242576]

(37). Ettinger A; van Haren J; Ribeiro SA; Wittmann T Doublecortin Is Excluded from Growing Microtubule Ends and Recognizes the GDP-Microtubule Lattice. Curr. Biol 2016, 26, 1549–1555. [PubMed: 27238282]

(38). Miller AL; Bement WM Regulation of Cytokinesis by Rho GTPase Flux. Nat. Cell Biol 2008, 11, 71–77 2008, 11 (1). [PubMed: 19060892]

(39). Skoufias DA; DeBonis S; Saoudi Y; Lebeau L; Crevel I; Cross R; Wade RH; Hackney D; Kozielski F S-Trityl-L-cysteine Is a Reversible, Tight Binding Inhibitor of the Human Kinesin Eg5 That Specifically Blocks Mitotic Progression. J. Biol. Chem 2006, 281, 17559–17569. [PubMed: 16507573]

(40). Oh E; Mark KG; Mocciaro A; Watson ER; Prabu JR; Cha DD; Kampmann M; Gamarra N; Zhou CY; Rape M Gene Expression and Cell Identity Controlled by Anaphase-Promoting Complex. Nature 2020, 579, 136–140. [PubMed: 32076268]

(41). Hayward D; Alfonso-Pérez T; Cundell MJ; Hopkins M; Holder J; Bancroft J; Hutter LH; Novak B; Barr FA; Gruneberg U CDK1-CCNB1 Creates a Spindle Checkpoint-Permissive State by Enabling MPS1 Kinetochore Localization. J. Cell Biol 2019, 218, 1182–1199. [PubMed: 30674582]

(42). Cazzalini O; Scovassi AI; Savio M; Stivala LA; Prosperi E Multiple Roles of the Cell Cycle Inhibitor P21CDKN1A in the DNA Damage Response. Mutat Res Rev Mutat Res 2010, 704, 12–20.

(43). Bunz F; Dutriaux A; Lengauer C; Waldman T; Zhou S; Brown JP; Sedivy JM; Kinzler KW; Vogelstein B Requirement for P53 and P21 to Sustain G2 Arrest after DNA Damage. Science 1998, 282, 1497–1501. [PubMed: 9822382]

(44). Jin P; Gu Y; Morgan DO Role of Inhibitory CDC2 Phosphorylation in Radiation-Induced G2 Arrest in Human Cells. J. Cell Biol 1996, 134, 963–970. [PubMed: 8769420]

(45). Lara-Gonzalez P; Moyle MW; Budrewicz J; Mendoza-Lopez J; Oegema K; Desai A The G2-to-M Transition Is Ensured by a Dual Mechanism That Protects Cyclin B from Degradation by Cdc20-Activated APC/C. Dev. Cell 2019, 51, 313–325 e10. [PubMed: 31588029]

(46). Norbury C; Blow J; Nurse P Regulatory Phosphorylation of the P34(Cdc2) Protein Kinase in Vertebrates. EMBO J. 1991, 10, 3321–3329. [PubMed: 1655417]

(47). Ayeni JO; Varadarajan R; Mukherjee O; Stuart DT; Sprenger F; Srayko M; Campbell SD Dual Phosphorylation of Cdk1 Coordinates Cell Proliferation with Key Developmental Processes in Drosophila. Genetics 2014, 196, 197–210. [PubMed: 24214341]

(48). Szmyd R; Niska-Blakie J; Diril MK; Renck Nunes P; Tzelepis K; Lacroix A; van Hul N; Deng LW; Matos J; Dreesen O; et al. Premature Activation of Cdk1 Leads to Mitotic Events in S Phase and Embryonic Lethality. Oncogene 2019, 38, 998–1018. [PubMed: 30190546]

(49). Alfieri C; Zhang S; Barford D Visualizing the Complex Functions and Mechanisms of the Anaphase Promoting Complex/Cyclosome (APC/C). Open Biol. 2017, 7, 170204. [PubMed: 29167309]

(50). de Boer HR; Guerrero Llobet S; van Vugt MATM Controlling the Response to DNA Damage by the APC/C-Cdh1. Cell. Mol. Life Sci 2016, 73, 949. [PubMed: 26650195]

(51). Liu Y; Cussiol JR; Dibitetto D; Sims JR; Twayana S; Weiss RS; Freire R; Marini F; Pellicioli A; Smolka MB TOPBP1Dpb11 Plays a Conserved Role in Homologous Recombination DNA Repair through the Coordinated Recruitment of 53BP1Rad9. J. Cell Biol 2017, 216, 623–639. [PubMed: 28228534]

(52). Sanford EJ; Comstock WJ; Faça VM; Vega SC; Gnügge R; Symington LS; Smolka MB Phosphoproteomics Reveals a Distinctive Mec1/ATR Signaling Response upon DNA End Hyper-Resection. EMBO J. 2021, 40, No. e104566. [PubMed: 33764556]

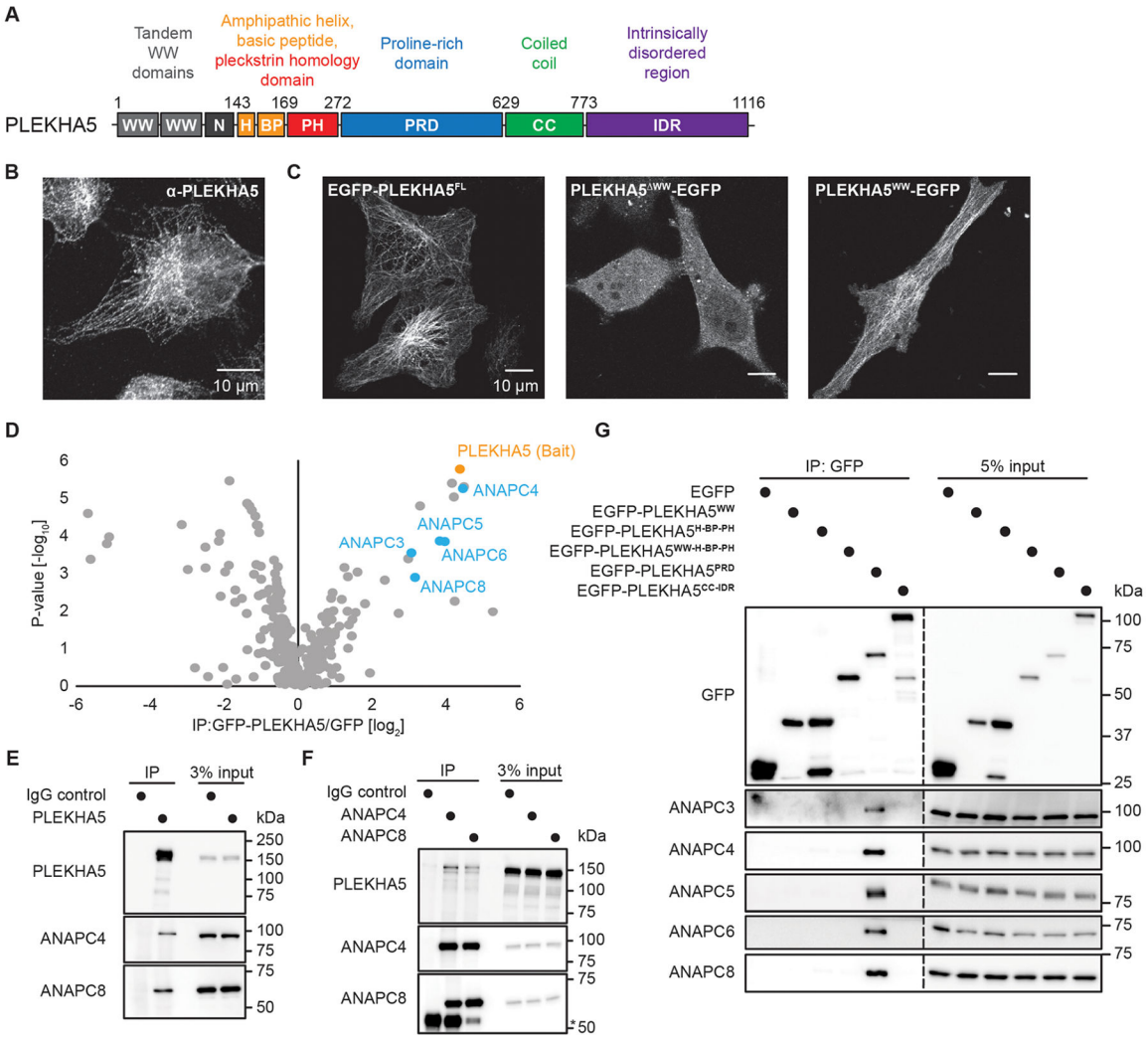

Figure 1.

PLEKHA5 localizes to the microtubule network and interacts with several APC/C subunits. (A) Domain map of PLEKHA5. (B) Immunofluorescence (IF) of endogenous PLEKHA5 in HeLa cells by confocal microscopy. (C) Confocal microscopy of HeLa cells transfected with different GFP-tagged PLEKHA5 constructs. (D) Volcano plot from SILAC MS proteomics experiments to determine the PLEKHA5 interactome, where proteins that are statistically significantly enriched in α-GFP immunoprecipitates from GFP-PLEKHA5-expressing HeLa cells compared to the IPs from GFP-expressing cells, including several APC/C subunits, appear on the top right. Statistical significance was determined by a Mann–Whitney *U* test. (E,F) Western blot analysis of co-IP experiments for endogenous PLEKHA5 (E) and the APC/C subunits ANAPC4 and ANAPC8 (F) to demonstrate the interaction between endogenous PLEKHA5 and the APC/C. IgG heavy chain from the IP is marked by an asterisk. (G) Truncation studies to reveal the PLEKHA5 PRD as sufficient to interact with APC/C.

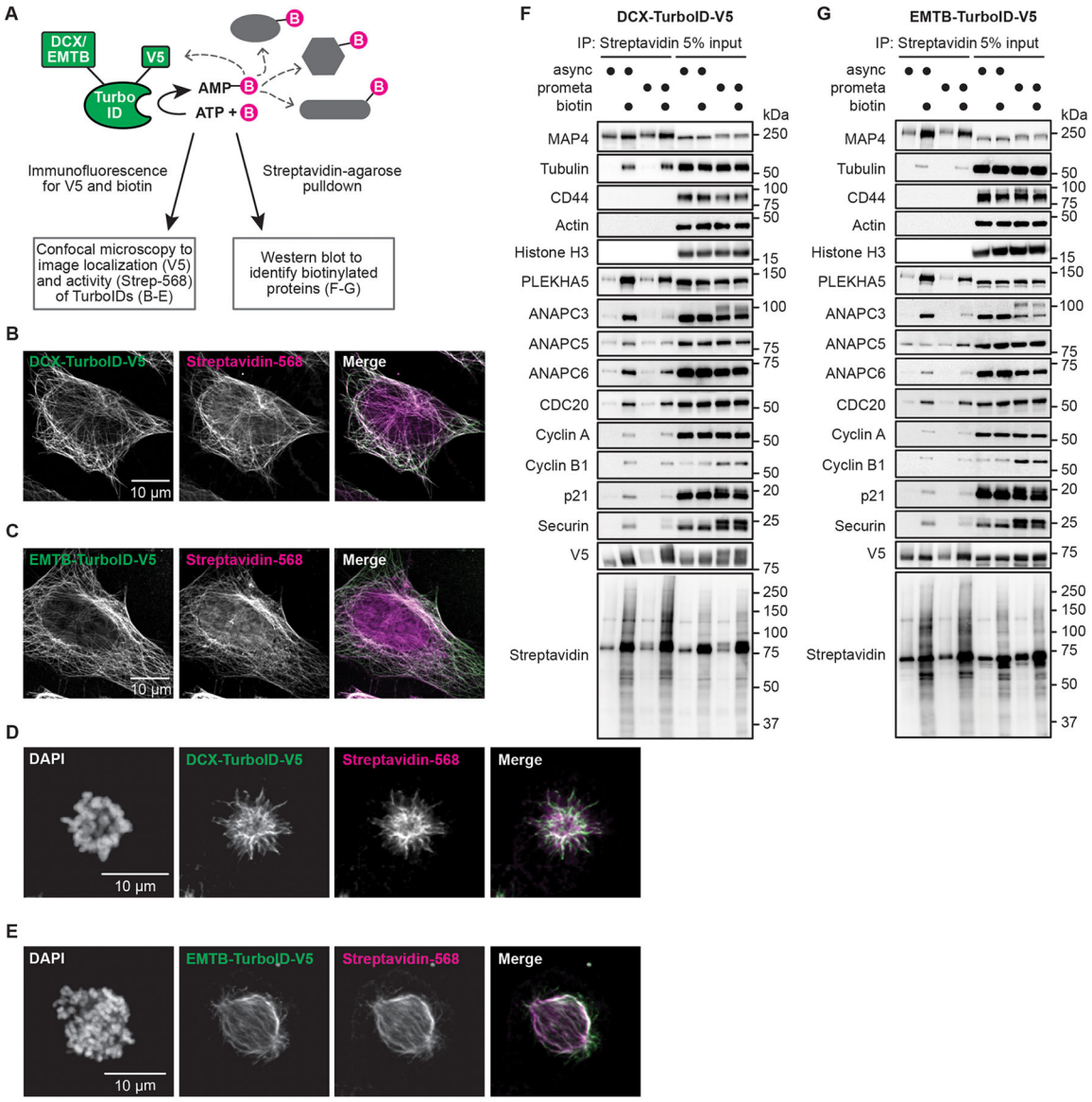

Figure 2.

Proximity biotinylation using microtubule-targeted TurboIDs reveals localization of endogenous PLEKHA5 and APC/C to the microtubule network. (A) Schematic representation of proximity biotinylation using MT-TurboID for visualization and identification of microtubule-associated proteins. (B–E) Both microtubule-targeting TurboID constructs exhibit the expected cellular localization and are active, as shown by staining against V5 (green) and biotin (streptavidin-Alexa Fluor 568, magenta) during interphase (B,C) and prometaphase (D,E). For (D,E), DAPI staining is indicated at left to show the expected chromosomal morphology of prometaphase, but for clarity, the merged image only contains the anti-V5 and streptavidin channels. (F,G) PLEKHA5, APC/C subunits, and APC/C substrates, but not markers of other subcellular locations, were biotinylated by microtubule-targeting TurboID constructs in both asynchronous and prometaphase-synchronized HeLa cells.

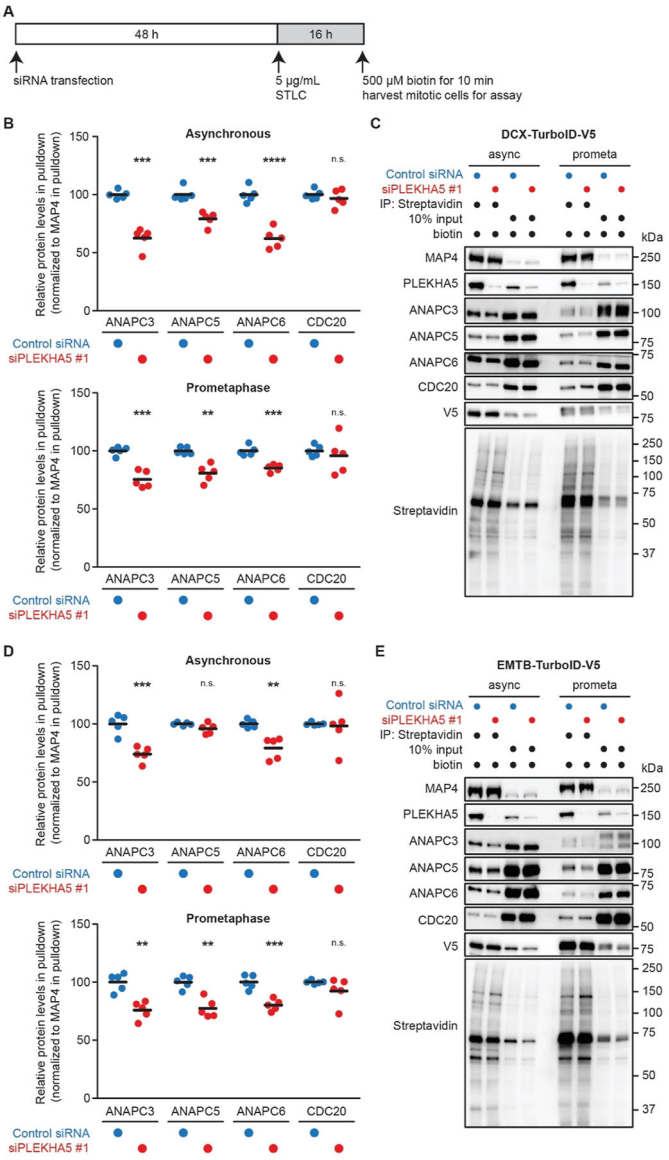

Figure 3.

PLEKHA5 knockdown causes a decrease in the association of APC/C, but not CDC20, with microtubules. (A) Schematic representation of the experimental timeline. (B–E) Knockdown of PLEKHA5 leads to reduced levels of APC/C subunits in streptavidin pulldowns from HeLa cells stably expressing DCX-TurboID-V5 (B,C) or EMTB-TurboID-V5 (D–E). Shown are the representative blots for the assay (C,E) and quantifications of protein levels (B,D) in streptavidin pulldowns ($n = 5$). Student's t-test: n.s. not significant; **$p < 0.01$; ***$p < 0.001$; ****$p < 0.0001$.

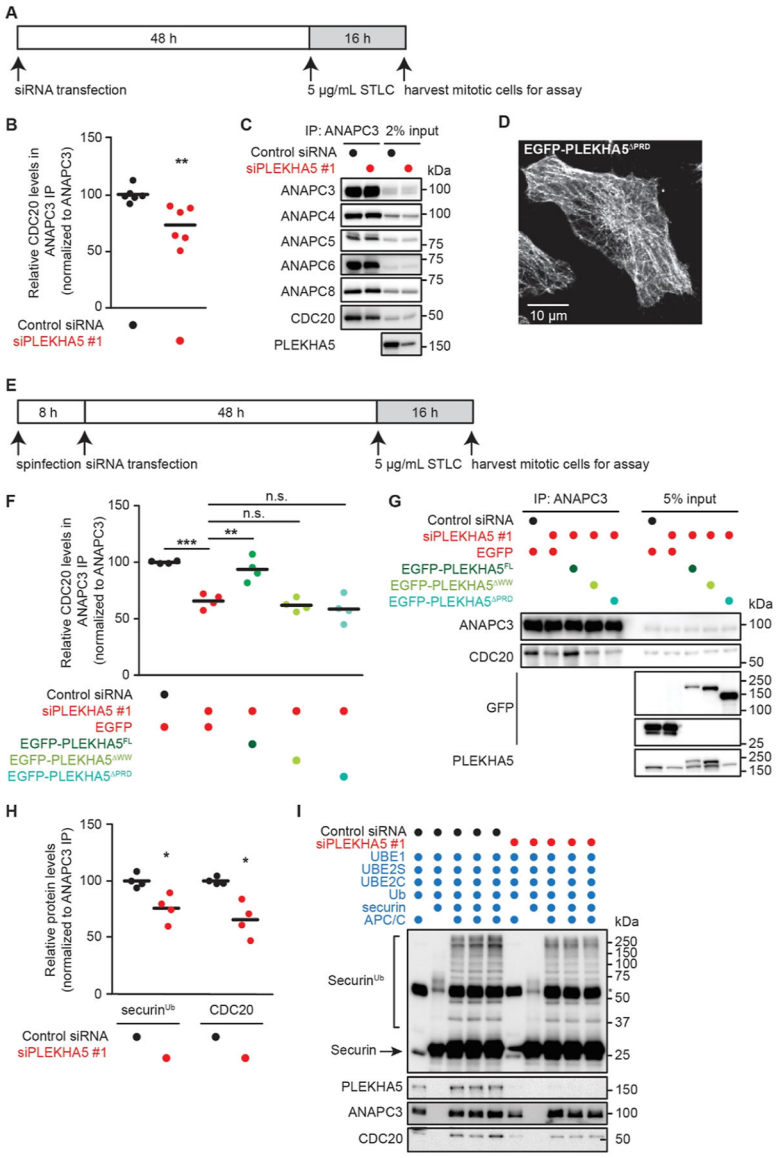

Figure 4.

PLEKHA5 knockdown reduces CDC20 loading of APC/C in prometaphase and diminishes the catalytic activity of APC/C. (A) Schematic representation of experimental timeline. Prometaphase cells were detached from the plate by gentle tapping and collected for use in assays. (B,C) siPLEKHA5 #1 treatment causes a decrease in APC/C association with CDC20. Shown are the representative western blot analysis of co-IP experiments for endogenous ANAPC3 (C) and quantification of CDC20 levels in IP samples (B) (n = 6). (D) Confocal microscopy analysis of EGFP-PLEKHA5$^{\Delta PRD}$, showing its microtubule localization. (E) Schematic representation of the experimental timeline for rescue experiments. (F,G) APC/C-CDC20 interaction can only be rescued by GFP-PLEKHA5^{FL}. Shown are quantification of CDC20 levels in IP samples (F) and representative western blots (G) (n = 4). We note that EGFP-PLEKHA5$^{\Delta PRD}$ expression was verified by the anti-GFP western blot because this construct does not contain the epitope recognized

by the PLEKHA5 antibody. (H,I) In vitro ubiquitination assays indicate that PLEKHA5 siRNA causes a reduction in APC/C E3 ligase activity. Shown are quantification of polyubiquitinated securin ($securin^{Ub}$) and CDC20 levels in the reactions (H) and representative western blots for the assay (I). IgG heavy chain from the APC/C purification is marked by an asterisk, and complete reactions (lanes 3–5 and 8–10) are shown in technical triplicate for each biological replicate ($n = 4$ biological replicates plotted in H). Student's t-test and ANOVA (one-way, Tukey): *$p < 0.05$; **$p < 0.01$, ***$p < 0.001$.

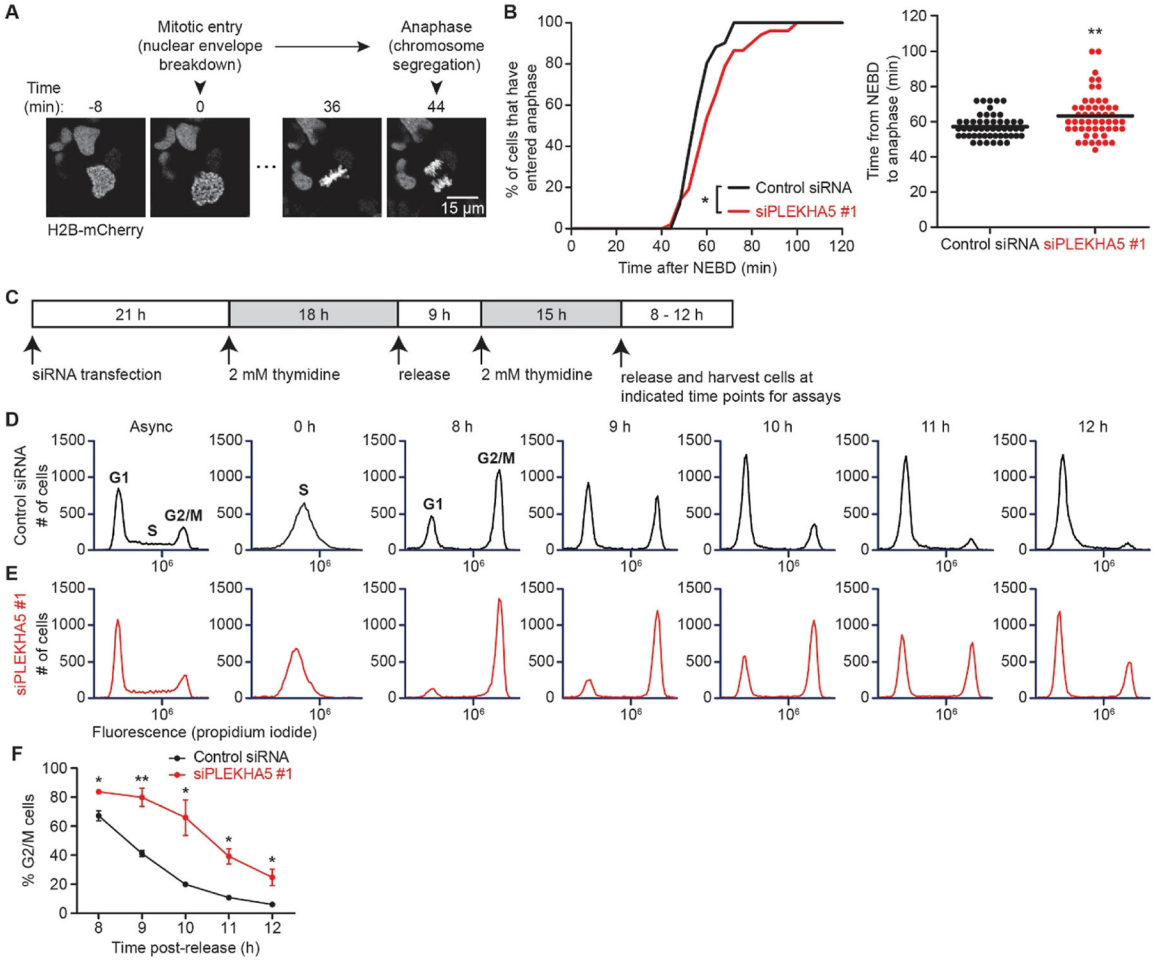

Figure 5.

PLEKHA5 knockdown delays mitotic progression and increases the fraction of cells in G2 and M phases. (A) Schematic representation of mitotic progression analysis in asynchronous HeLa cells by time-lapse, live-cell imaging of H2B-mCherry. (B) Quantification of mitosis progression in asynchronous HeLa cells, with time from NEBD to anaphase plotted as cumulative frequency (left, Kolmogorov–Smirnov test) and scatter plot (right, Mann–Whitney *U* test) ($n = 50–51$ cells): *$p < 0.05$; **$p < 0.01$. (C) Schematic representation of the experimental timeline using a double thymidine block (DTB). (D–F) siPLEKHA5 #1 treatment leads to the accumulation of HeLa cells in the G2 and M phases. DNA content of asynchronous (async) or DTB-synchronized/released HeLa cells transfected with control siRNA (D) or siPLEKHA5 #1 (E) were evaluated by PI staining and flow cytometry analysis, and the percentage of cells in G2 and M phases was quantified and shown in (F) ($n = 3$). Student's *t*-test: *$p < 0.05$; **$p < 0.01$.

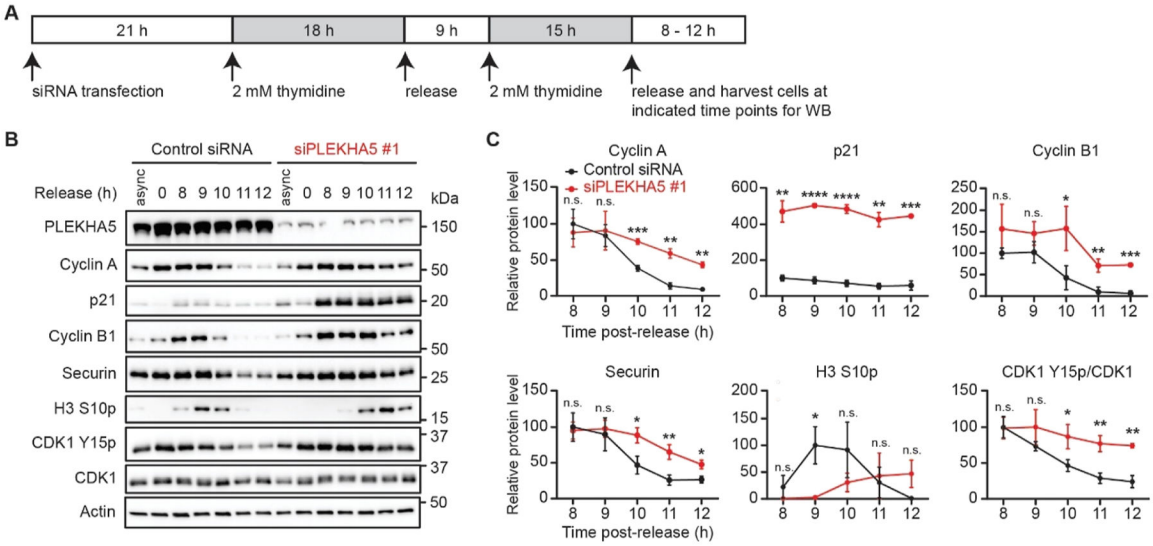

Figure 6.

PLEKHA5 knockdown causes a buildup of APC/C substrates. (A) Schematic representation of the experimental timeline. (B,C) APC/C substrates and G2/M protein markers persist in cells treated with siPLEKHA5 #1. Shown are representative western blots (B) and quantification of protein levels (C) of lysates from HeLa cells subject to control siRNA or siPLEKHA5 #1 ($n = 3$). Student's t-test: n.s. not significant; *$p < 0.05$; **$p < 0.01$; ***$p < 0.001$; ****$p < 0.0001$.

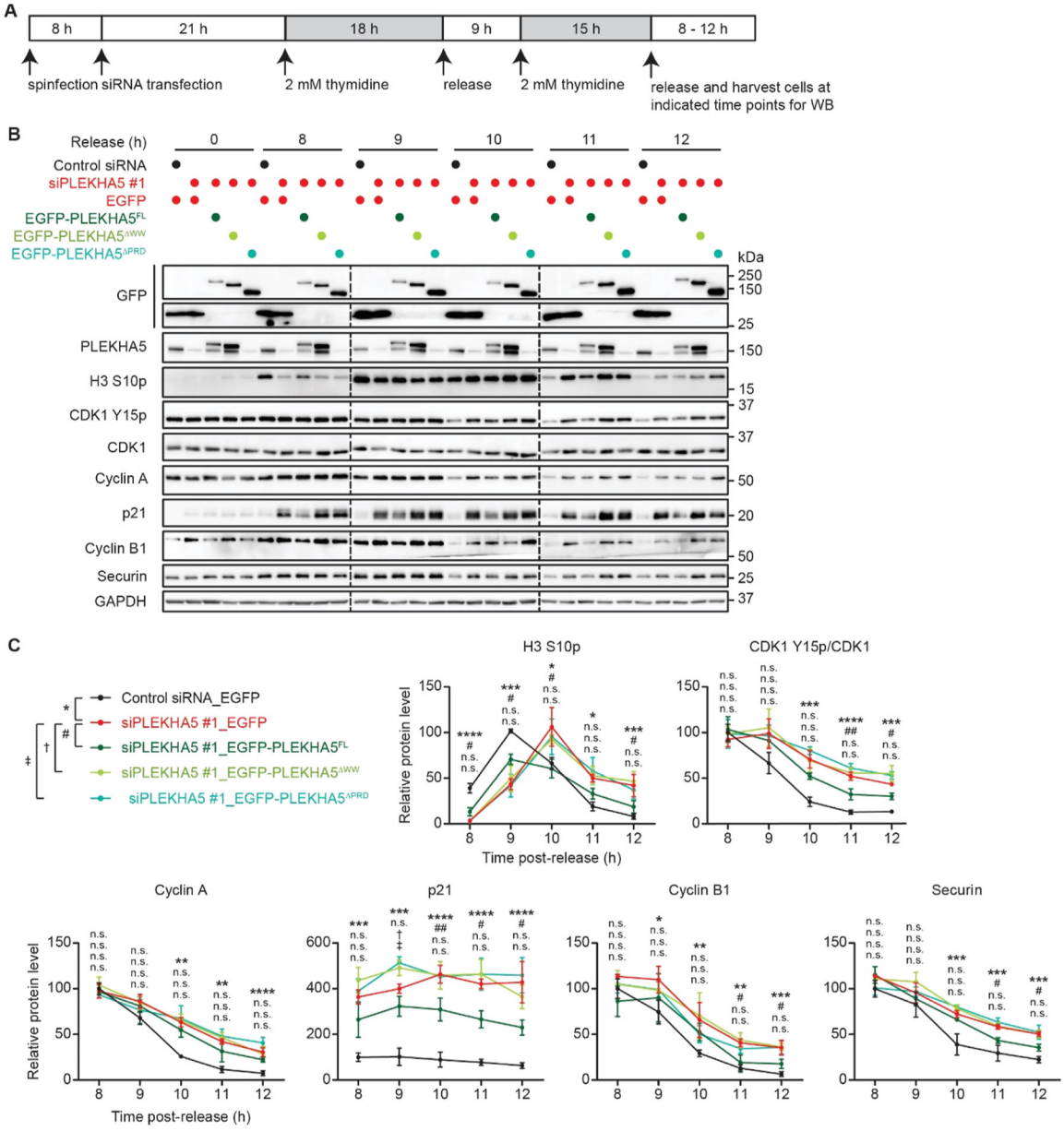

Figure 7.

PLEKHA5–APC/C interaction at microtubules is required to rescue the accumulation of mitosis markers and APC/C substrates induced by PLEKHA5 knockdown. (A) Schematic representation of the experimental timeline. (B,C) Accumulation of mitosis markers and APC/C substrates in siPLEKHA5 samples is partially rescued by exogenous expression of EGFP-PLEKHA5^{FL} but not EGFP-PLEKHA5$^{\Delta WW}$ or EGFP-PLEKHA5$^{\Delta PRD}$. Shown are representative western blots (B) and quantification of protein levels (C) in HeLa cells transduced with conditioned media containing lentivirus encoding EGFP, siRNA-resistant EGFP-PLEKHA5^{FL}, siRNA-resistant EGFP-PLEKHA5$^{\Delta WW}$, and siRNA-resistant EGFP-PLEKHA5$^{\Delta PRD}$ by spinfection (n = 3). Notes: EGFP-PLEKHA5$^{\Delta PRD}$ expression is verified by GFP blot because this construct does not contain an epitope recognized by the PLEKHA5

antibody. ANOVA (one-way, Tukey): n.s. not significant; *, #, † and ‡$p < 0.05$; **, ##, †† and ‡‡$p < 0.01$; ***, ###, ††† and ‡‡‡$p < 0.001$; ****, ####, †††† and ‡‡‡‡$p < 0.0001$.

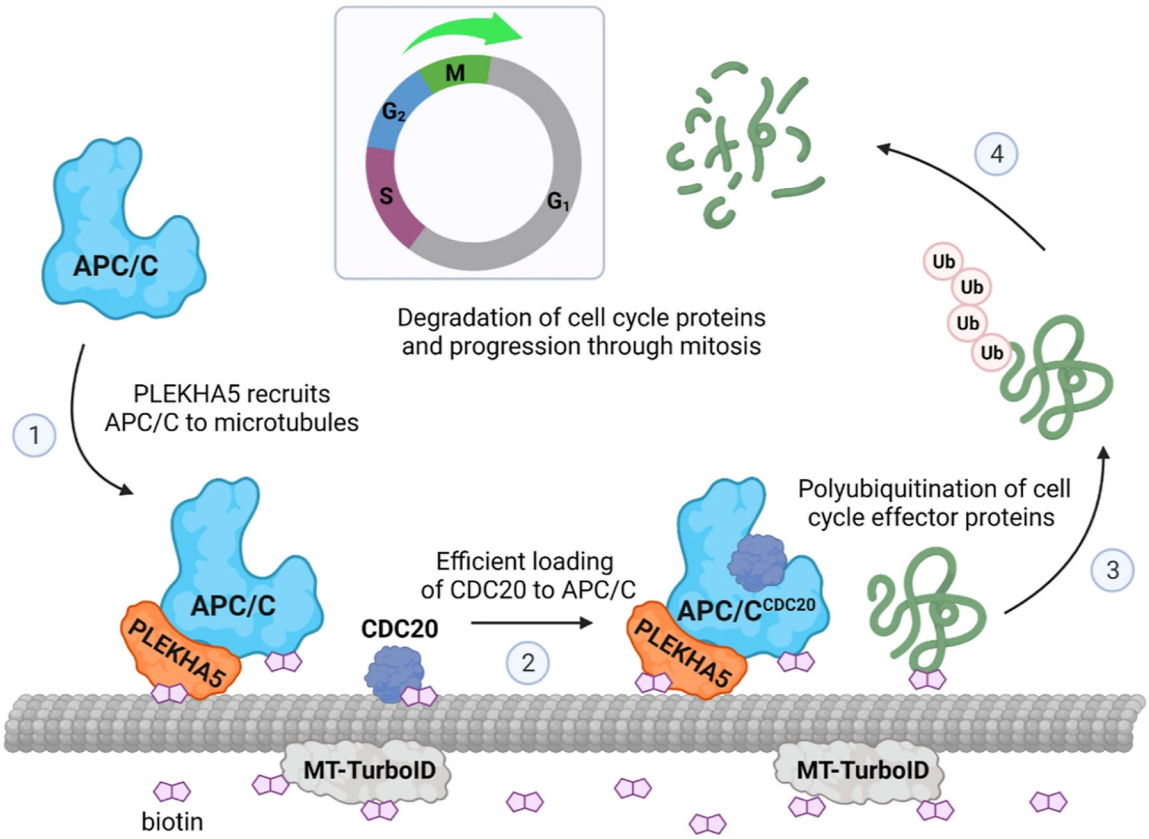

Figure 8.

Model for PLEKHA5 function in mitosis as a microtubule-localized adaptor that regulates the spatial organization of the APC/C E3 ubiquitin ligase. PLEKHA5 is a microtubule-resident protein that recruits a pool of APC/C to the microtubule cytoskeleton, as demonstrated by its biotinylation by microtubule-localized proximity labeling tools (MT-TurboID), thus increasing the local concentration of APC/C along the microtubule network. Upon mitotic phosphorylation, this pool of APC/C can efficiently interact with its coactivator CDC20 and subsequently polyubiquitinate its mitotic substrates. In this manner, PLEKHA5 organizes APC/C in space to facilitate the timely turnover of key mitotic proteins to promote progression through mitosis (figure and TOC graphic created with BioRender).